AIChE

# Computational Study of Staged Membrane Reactor Configurations for Methane Steam Reforming. II. Effect of Number of Stages and Catalyst Amount

**Alessio Caravella, Francesco Paolo Di Maio, and Alberto Di Renzo**
Dept. of Chemical and Materials Engineering, University of Calabria, Rende (CS), Italy

*DOI 10.1002/aic.11960*
*Published online August 20, 2009 in Wiley InterScience (www.interscience.wiley.com)*

*The present work complements part I of this article and completes a computational analysis of the performances of staged membrane reactors for methane steam reforming. The influence of the number of stages and catalyst amount is investigated by comparing the methane conversion and hydrogen recovery yield achieved by an equisized-staged reactor to those of an equivalent conventional membrane reactor for different furnace temperatures and flow configurations (co- and counter-current). The most relevant result is that the proposed configuration with a sufficiently high number of stages and a significantly smaller catalyst amount (up to 70% lower) can achieve performances very close to the ones of the conventional unit in all the operating conditions considered. This is equivalent to say that the staged configuration can compensate and in fact substitute a significant part of the catalyst mass of a conventional membrane reactor. To help the interpretation of these results, stage-by-stage temperature and flux profiles are examined in detail. Then, the quantification of the performance losses with respect to the conventional reactor is carried out by evaluating the catalyst amount possibly saved and furnace temperature reduction.* © 2009 American Institute of Chemical Engineers *AIChE J,* 56: 259–267, 2010
*Keywords: staged membrane reactor, catalyst distribution, methane steam reforming*

## Introduction

In Part I of this work,[1] the methane steam reforming process to produce high purity hydrogen was considered to be carried out in a staged membrane reactor (SMR) with two and 10 stages. That analysis highlighted the role held by different catalyst axial distributions achieved by maximizing the hydrogen recovery yield and methane conversion. The optimization of the performance indices was performed by setting the stage lengths as design variables and considering constant number of stages and catalyst amount. To the authors' knowledge, in the literature the effect of these two operating parameters has not been studied specifically. However, as it will be shown throughout the article, their influence on the process can be relevant, also in the perspective of reducing the reactor operating costs. Several research groups considered or used in their works a SMR,[2–5] but the number of stages was set in all the cases as a fixed parameter. Li et al.[6] carried out a simulation work for methane steam reforming investigating a staged Pd-membrane reactor (MR), where two reactive and two separative stages were placed in two different furnaces, each one with its temperature. In particular, they investigated the role of the amount of membrane area present in the separative stages and the influence of other operating variables on the performances of the overall process. In the simulation work of Jordal et al.[7]

Correspondence concerning this article should be addressed to A. Caravella at alessio.caravella@unical.it

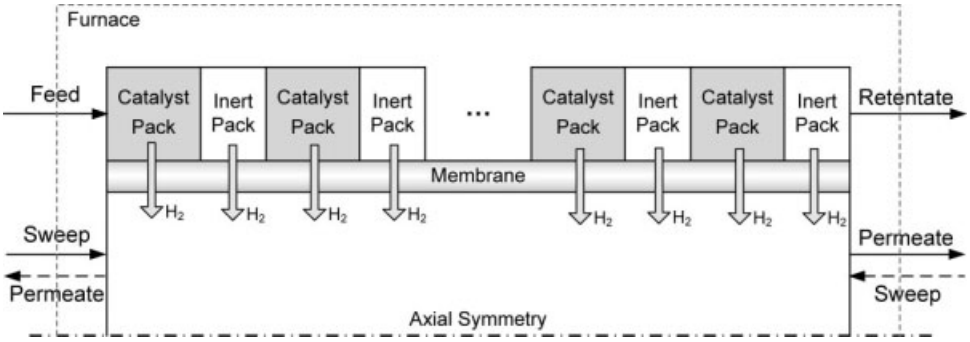


**Figure 1. Scheme of the equisized SMR considered.**

concerning the possibility of integrating $H_2$ selective membrane-based technology in a gas turbine process for $CO_2$ capture, a reformer with five reactive stages and five separative membrane stages was considered, choosing the number of stages according with computational considerations.

The aim of this article is to analyze by computer modeling the role played by the number of stages and the catalyst amount in changing the SMR performances. The assessment of the process characteristics will be carried out in terms of overall indices such as hydrogen recovery factor, recovery yield, and methane conversion.

## Description of the System

Methane steam reforming is considered to be carried out in an SMR, where reactive stages are in series with inert ones (Figure 1). The stage lengths can in principle be different, even optimal stage length distributions could be obtained to achieve maximum conversion or hydrogen recovery.[1,8] However, as the number of stages ($n^{Stages}$) increases, the optimization of individual stage lengths becomes meaningless. Hence, equisized stages are considered. Although the characteristics of the system have been already as reported in Part I of this work,[1] its main geometrical data are recalled here for clarity (Table 1).

The kinetic mechanism of methane steam reforming on Ni-based catalyst is taken from the work of Xu and Froment.[9,10] The permeation properties of the membrane considered (Pd-alloy) are obtained from the experimental studies of Tong et al.[11,12] The details about the mathematical model of the system and its validation are reported elsewhere.[1,8] The number of stages $n^{Stages}$ and catalyst amount $y$ in the reactor represent the main investigation variables of this work. The latter will denote a fraction of the total amount present in an equivalent fully filled MR of the same size.

The value of $y$ and the one of the length of the reactor stages (inert and reactive) are strictly related to each other. In fact, the expression "equisized" refers to the reactive stages and to the inert ones distinctly. An inert and a reactive stage have in general different lengths, except when $y = 50\%$. Formally, the lengths of the reactive and inert stages can be expressed as a function of $y$ and $n^{Stages}$ by:

$$l^R = \frac{y l^{Tot}}{n^R}, \quad l^I = \frac{(1-y) l^{Tot}}{n^I}, \quad l^{Tot} = \text{constant}$$
$$\frac{l^R}{l^I} = \frac{y}{1-y}, \quad n^R = n^I = \frac{n^{Stages}}{2} \tag{1}$$

where $l$ is the length and the superscripts "$R$" and "$I$" are the "reactive" and "inert" stage, respectively. Several furnace temperatures ($T^{Furnace}$) and both co- and counter-current configuration will be considered. The reactor performances are evaluated by means of the indices whose definitions are reported in Table 2.

**Table 1. Geometrical Data of the System**

| $ID^{Tube}$ (mm) | $\delta^{Mem}$ ($\mu$m) | $ID^{Shell}$ (mm) | $OD^{Shell}$ (mm) | $L^{Tot}$ (cm) | $d_p$ ($\mu$m) |
|---|---|---|---|---|---|
| 10 | 6 | 30 | 32 | 100 | 400 |

## Analysis of the Reactor Performances

### *Overall reactor performances*

Simulations are carried out for a reactor operated at 400, 500, and 600°C, and under a typical $H_2O/CH_4$ feed ratio, as reported in Table 3. In Figures 2 and 3, the SMR performances are shown as functions of $n^{Stages}$ for various values of $y$ at 600 and 500°C, respectively. The minimum $n^{Stages}$ considered here is 10, whereas the maximum one is 100. The latter extreme is impractical to achieve in real systems and, therefore, is used essentially to represent the asymptotic trend of the reactor performances as the number of stages increases.

To discuss the system behavior, let us first focus on the case of $y = 30\%$ at 600°C (Figure 2). It can be observed that the curves relative to $x$ and RY show a continuous increase, whilst RF decreases, although not very strongly. This trend results from a complex combination of effects mainly due to the heat transfer throughout the sequence of stages. In each couple of reactive-inert stages, the reactive

**Table 2. Definition of the Performance Indices**

| Factor | Description | Formal Definition | Mathematical Definition |
|---|---|---|---|
| $x$ | $CH_4$ conversion | $\frac{CH_4 converted}{CH_4 fed}$ | $1 - \frac{F^{Ret}_{CH_4}}{F^{0}_{CH_4}}$ |
| $RF$ | $H_2$ recovery factor | $\frac{H_2 recovered in the permeate side}{H_2 produced}$ | $\frac{F^{Perm}_{H_2}}{F^{Ret}_{H_2}+F^{Perm}_{H_2}}$ |
| $RY$ | $H_2$ recovery yield | $\frac{H_2 recovered in the permeate side}{Maximum H_2 produced at total CH_4 conversion}$ | $\frac{F^{Perm}_{H_2}}{4F^{0}_{CH_4}}$ |

**Table 3. Operating Conditions**

| Side | Pressure (kPa) | | | | | | Total Flow Rate (mmol/s) |
|---|---|---|---|---|---|---|---|
| | $H_2$ | $CH_4$ | $CO_2$ | $H_2O$ | CO | Total | |
| Feed | – | 125 | – | 375 | – | 500 | 8 |
| Sweep | – | – | – | 120 | – | 120 | 8 |

$T^{Furnace} = \{400; 500; 600\}$°C.

stream is involved in a ''thermal cycle'' where temperature is first decreased because of the reaction and then continuously increased in the inert stages. When considering large stages (low $n^{Stages}$) in the last part of the reactive zones the temperature is low because of the reaction. This, in turn, lowers the reaction rate and the permeating flux. At a higher $n^{Stages}$, the reactive stream can exploit a better thermal condition, as the stage-by-stage profiles analysis will demonstrate below (Stage-by-Stage Profiles section).

These circumstances favor the reaction rate and, thus, all the performance indexes measuring the productivity of the reactor, i.e. $x$ and recovery yield. They also act positively on the permeation properties, but to a lesser extent. Therefore, the recovery factor, which measures the ratio between the permeated over produced hydrogen, is slightly penalized by a high $n^{Stages}$. For the conversion and recovery yield, the influence of $n^{Stages}$ is relevant for a catalyst fraction less than about 50%.

On increasing the catalyst amount above 50%, there is no appreciable difference among low and high $n^{Stages}$, because the presence of more catalyst compensates its nonoptimal use. As it will be discussed in ''Gain Maps for the Staged Membrane Reactor'' section, this concept is particularly important, because it shows that a proper reactor design can

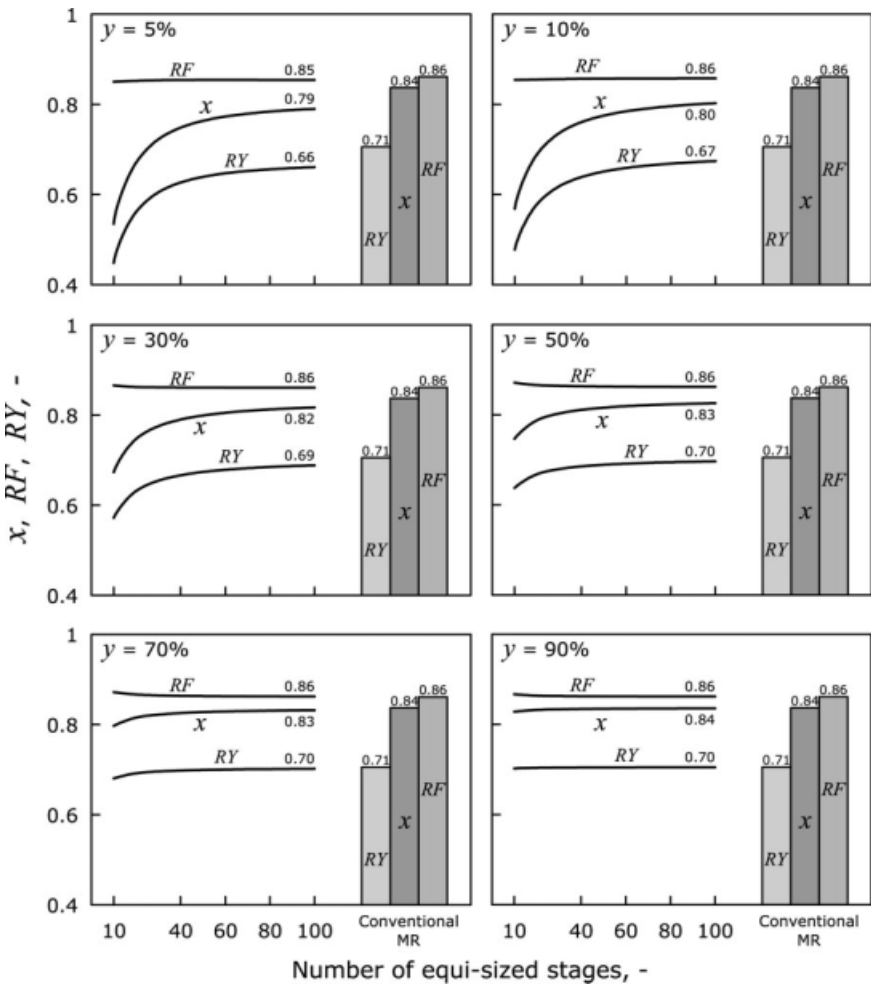


**Figure 2. Performances of the SMR ($CH_4$ conversion, $H_2$ recovery factor and $H_2$ recovery yield) in co-current flow as a function of $n^{Stages}$ for different percentages of catalyst at $T^{Furnace} = 600$°C.**

The performances of the conventional MR are reported for comparison. The remaining operating conditions are specified in Table 3.

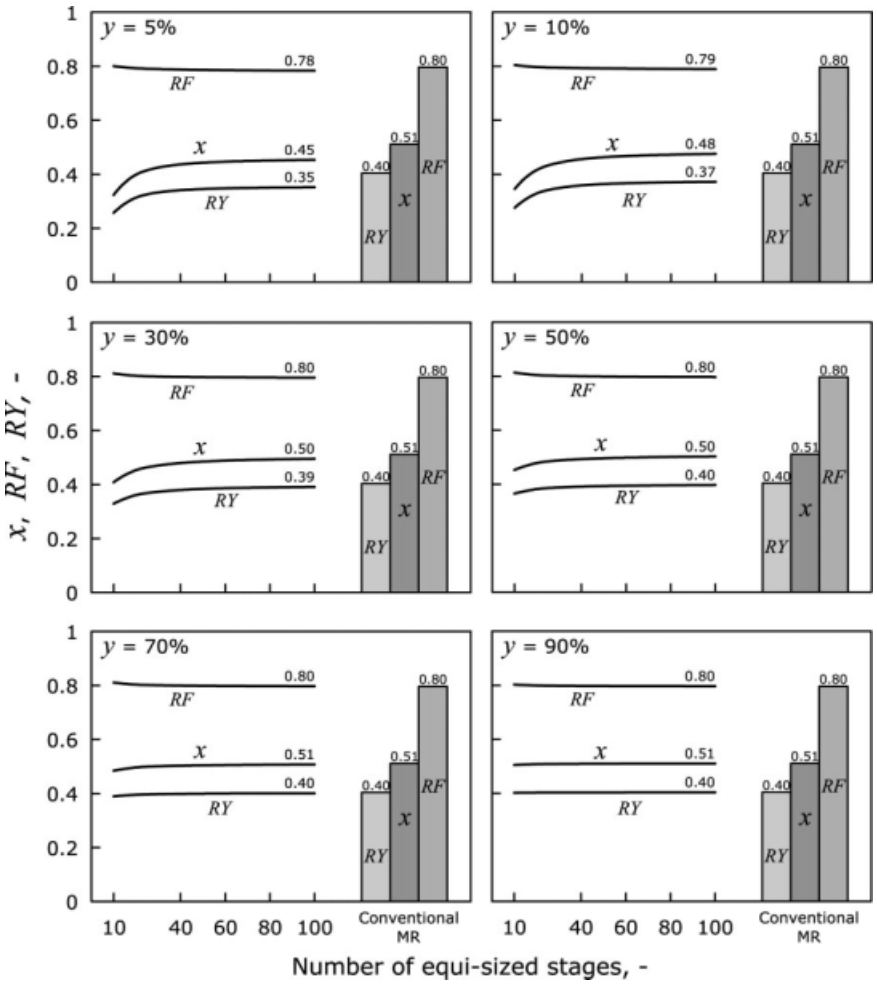


**Figure 3. Performances of the SMR ($CH_4$ conversion, $H_2$ recovery factor and $H_2$ recovery yield) in co-current flow as a function of $n^{Stages}$ for different percentages of catalyst at $T^{Furnace}$ = 500°C.**

The performances of the conventional MR are reported for comparison. The remaining operating conditions are specified in Table 3.

lead to performances analogous to a conventional MR but with a smaller catalyst amount. The results of Figures 2 and 3 also show that the number of stages at which a plateau is reached depends on the catalyst amount considered. At 500°C, the qualitative behavior of the profiles remains unchanged, but their dependence on $n^{Stages}$ and on $y$ becomes less significant than at 600°C (Figure 3). This occurs because the reaction is favored by a high temperature by both thermodynamics and kinetics. The overall result of this is that, for a slower reaction rate (due to a lower $T^{Furnace}$), a certain part of advantage in using a higher $n^{Stages}$ and/or a larger $y$ for achieving higher performances is lost. The influence of a counter-current configuration is shown in Figure 4, where the results for the overall indices at $y = 30\%$ for $T^{Furnace}$ of 400, 500, and 600°C are reported in comparison with those of the corresponding MR. The trends are analogous to the co-current case, though the quantitative values are higher.

By carefully examining the performance of the counter-current configuration, it can be observed that the recovery factor is more sensitive to $n^{Stages}$. This could be due to the more uniform hydrogen driving force profiles than the co-current configuration.

### *Stage-by-stage profiles*

To acquire a deeper understanding of the influence of using a staged configuration on the overall reactor performance, it is useful to analyze the stage by stage profiles of the most relevant variables involved in. Only two significant catalyst fractions values (20 and 50%), one $T^{Furnace}$ (600°C), and co-current configuration will be considered to keep the analysis treatable. One of the most relevant variables is the local temperature developing along the reactor in the reaction side (Figure 5).

It results from the complex interaction of heat transfer to the furnace and to the permeate side and the heat absorbed by the highly endothermic reaction. As shown in Figure 5, the effect of an increasing $n^{Stages}$ is to lead the stage-by-stage profile closer to the MR one. Thus, the profiles along the reactor allow demonstrating the improvement due to the inert stages inter-laid between reactive stages. Their key-role is to act as inter-recharge of energy that will be exploited particularly in the subsequent reaction stage. With few stages, the initial reaction temperature is very high but decreases quickly as much as the reaction proceeds. With

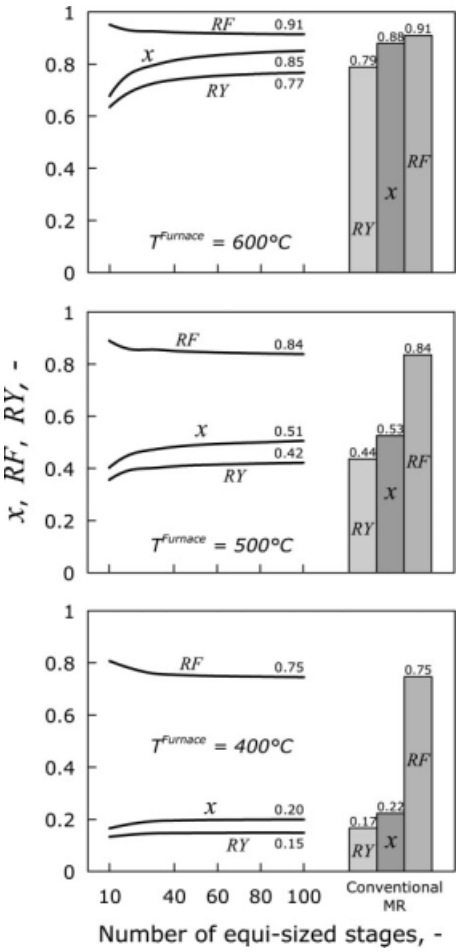


**Figure 4. Performances of the SMR ($CH_4$ conversion, $H_2$ recovery factor, and $H_2$ recovery yield) in counter-current flow as a function of $n^{Stages}$ for several $T^{Furnace}$ at a $y$ of 30%.**

The performances of the conventional MR are also reported for comparison. The remaining operating conditions are specified in Table 3.

many stages the reaction starts at a temperature slightly lower but that does not decrease significantly. The resulting thermal conditions are more favorable, contributing to lead to a higher conversion. This is demonstrated in Figure 6, where the average temperatures calculated in each reactive stage are shown for 10 and 100 stages. It is clearly shown that the parts of the profiles characterized by higher temperatures (Figure 5) do not provide a significant contribution.

The difference between 10 and 100 stages profile increases as a smaller amount of catalyst is considered (Figure 6a vs. Figure 6b). As it will be confirmed below, this indicates that the lower the catalyst fraction, the larger is the advantage of using a high number of stages.

An analogous behavior can be observed also in terms of hydrogen permeation through the membrane.

By an analysis of the permeating flux (Figure 7), it is even more evident that a high $n^{Stages}$ provides more favorable conditions for better performances. In fact, the hydrogen flux appears more "uniformly" distributed along the reactor

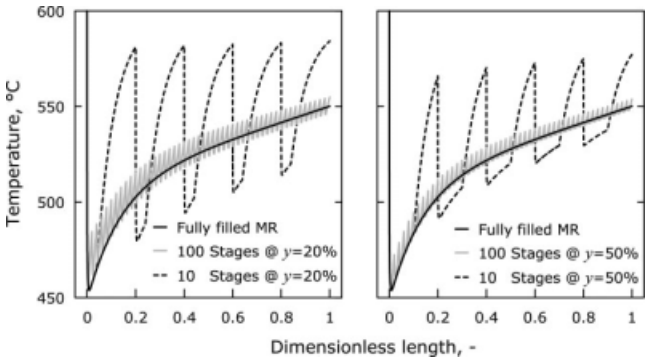


**Figure 5. Temperature profiles in the reaction side for several $n^{Stages}$ and y in co-current flow at $T^{Furnace}$ = 600°C.**

The remaining operating conditions are specified in Table 3.

and even the local fluxes are higher than the lower number of stages case. Therefore, the resulting hydrogen recovered in the permeate is higher.

It is instructive to examine the profiles of the performance indices along each stage. Figure 8 shows the conversion increase along the reactor for three values of $n^{Stages}$ at $y = 20\%$ and two values at $y = 50\%$.

Analyzing the behavior of the conversion profiles (Figure 8) for three values of $n^{Stages}$ at $y = 20\%$, it can be observed that in the initial part of the system the reaction is very rapid and the distributions achieve almost the same performances. After this zone, the differences between the distributions considered increase progressively towards the reactor outlet. When considering 50% of catalyst, these differences decrease. This clearly indicates that the lower is the catalyst amount the more significant is the influence of its distribution. Analogous considerations can be made for the hydrogen recovery yield (Figure 9), which is also favored by a high $n^{Stages}$. It is important to remark that a general trend able to be observed in Figures 8 and 9 is that the lower the catalyst amount used, the higher the beneficial effect of an increased number of stages.

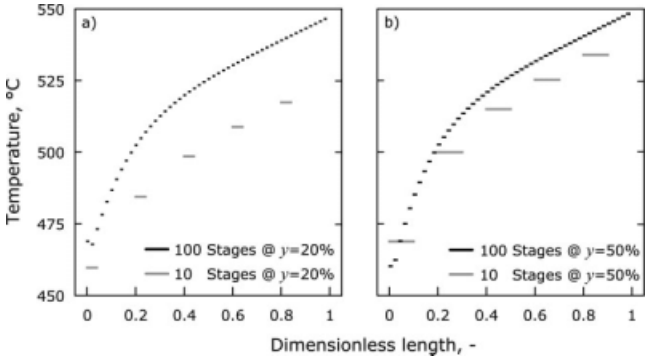


**Figure 6. Average temperature calculated in the reaction side of the reactive stages for two $n^{Stages}$ and $y$ in co-current flow at $T^{Furnace}$ = 600°C.**

The remaining operating conditions are specified in Table 3.

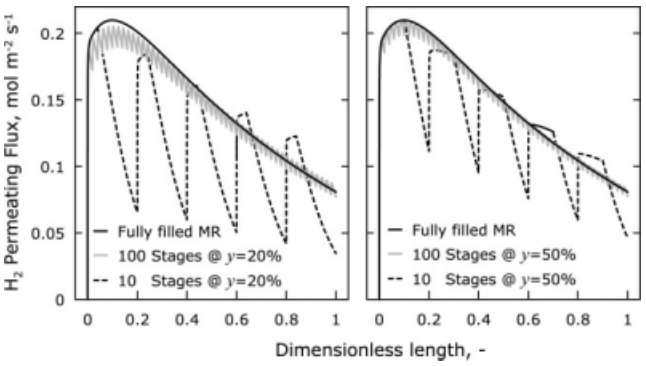


**Figure 7. Hydrogen permeating flux profiles for several $n^{Stages}$ and $y$ in co-current flow at $T^{Furnace}$ = 600°C.**

The remaining operating conditions are specified in Table 3.

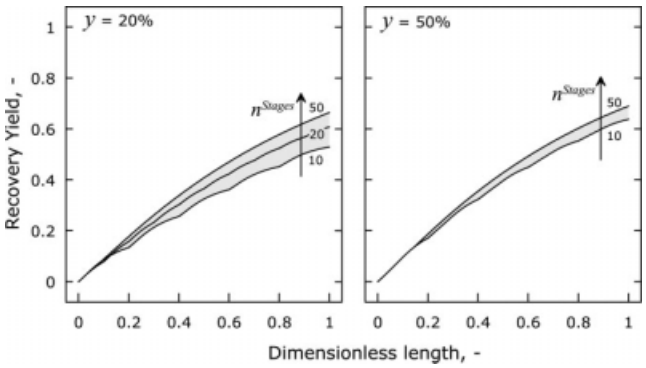


**Figure 9. Recovery yield profiles for some $n^{Stages}$ and $y$ in co-current flow at $T^{Furnace}$ = 600°C.**

The remaining operating conditions are specified in Table 3.

### *Uniform vs. staged catalyst distribution*

The previous analysis clearly showed the significant advantage of adopting a staged catalyst distribution with an $n^{Stages}$ as high as possible. However, it has already been pointed out that, as $n^{Stages}$ increases, the difficulty of assembling such a reactor becomes progressively larger. In these conditions, the reactive and inert stages tend to be vanishingly small and infinitely close to each other. From a physical point of view, this situation should be very similar to one in which inert and catalytic pellets are placed in the same portion of volume, i.e., it should tend towards a uniform distribution of the given catalyst among inert pellets (Figure 10).

Computer simulations have been carried out to verify this condition by changing, in the model equations, the kinetic law to account for the presence of a reduced catalyst amount in the target volume where the mass and energy balances are written. This was made by multiply the reaction rate term by the catalyst fraction $y$. Table 4 lists the simulation results obtained considering a staged distribution with 100 stages in comparison to the ones of a reactor where the catalyst is uniformly distributed.

Calculations have been carried out for all the operating conditions considered previously. However, only the case in co-current at 600°C is reported, as the results for the other cases are completely analogous. As it is possible to notice, the difference between the staged distribution and the uniform one is absolutely negligible for every performance index. Obviously, this gap tends to decrease as a higher $y$ is considered, because in the trivial case of a $y$ of 100% the two reactors are coincident. In summary, the considerations made for an SMR with a sufficiently high $n^{Stages}$ are also valid for a MR where catalytic and inert pellets are uniformly distributed.

## Gain Maps for the SMR

The beneficial effect of the SMR over a conventional MR is most conveniently examined in terms of savings achievable for a given performance target. So, let us examine the performances of a 100-staged reactor as a function of $y$ and compare it to the conventional MR, considering a $T^{Furnace}$ of 400, 500, and 600°C (Figure 11). It is to be noticed that, although the curves are similar to those in Figures 2–4, in this case the role of $n^{Stages}$ and $y$ is reverted. Quite obviously all indices increase as $y$ is increased, but the most important conclusion we can draw from Figure 11 is that, between about 30 and 50% of the catalyst, in all cases the performances of the staged system are still comparable with those of the reference MR. This means that, using an SMR, there is

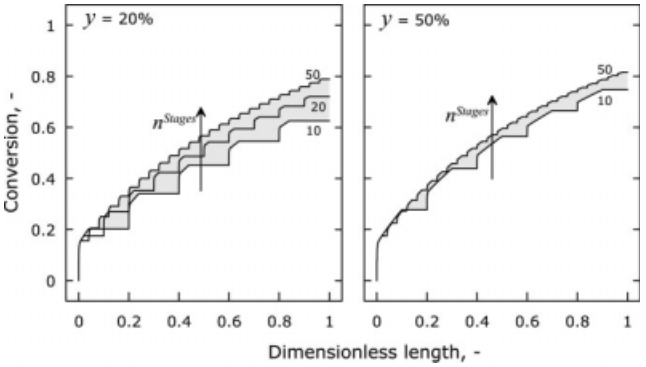


**Figure 8. Conversion profiles for $n^{Stages}$ and $y$ in co-current flow at $T^{Furnace}$ = 600°C.**

The remaining operating conditions are specified in Table 3.

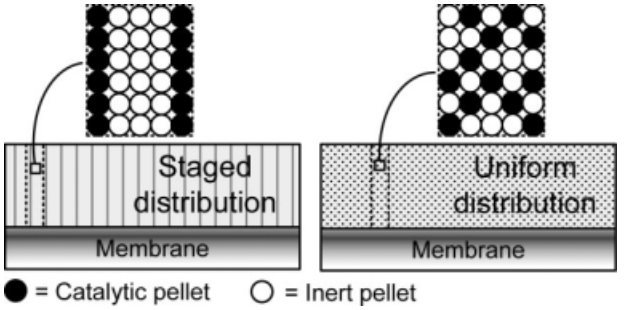


**Figure 10. Sketch of the MR with a uniform catalyst distribution, being equivalent to a staged membrane with the same amount of catalyst for sufficiently high number of stages.**

**Table 4. Comparison Among the Performance Indices Corresponding to Two-Staged Distributions ($n^{Stages}$ of 50 and 100) and a Uniform One as a Function of the Catalyst Fraction in Cocurrent Flow**

| | Staged Distributions | | | | | | | | |
|---|---|---|---|---|---|---|---|---|---|
| | $n^{Stages} = 50$ | | | $n^{Stages} = 100$ | | | Uniform Distribution | | |
| $y$ (%) | $x$ | RF | RY | $x$ | RF | RY | $x$ | RF | RY |
| 10 | 0.775 | 0.857 | 0.651 | 0.803 | 0.857 | 0.674 | 0.819 | 0.856 | 0.686 |
| 30 | 0.799 | 0.861 | 0.674 | 0.817 | 0.861 | 0.689 | 0.832 | 0.860 | 0.700 |
| 50 | 0.816 | 0.863 | 0.689 | 0.826 | 0.862 | 0.697 | 0.835 | 0.861 | 0.703 |
| 70 | 0.828 | 0.863 | 0.699 | 0.832 | 0.862 | 0.702 | 0.836 | 0.861 | 0.704 |
| 90 | 0.835 | 0.862 | 0.705 | 0.836 | 0.862 | 0.705 | 0.837 | 0.861 | 0.705 |

$T^{Furnace} = 600°C$.

no need to fill it with catalyst to get the same result as the conventional MR and this may represent a considerable economical advantage.

In this way, the amount of catalyst possibly saved using a staged reactor can be evaluated as a function of the performance decrease (Figure 12). By carefully examining the profiles at different conditions and flow configurations, it can be noticed that the slope of the lines is very high at the lowest performance gaps, especially at high temperatures, i.e. when higher performances are achieved. Another interesting fact is that the difference between co- and counter current case is so little that, in a first approximation, it is possible to use equivalently only one of these plots to evaluate the catalyst amount saved. This fact cannot be predicted a priori by

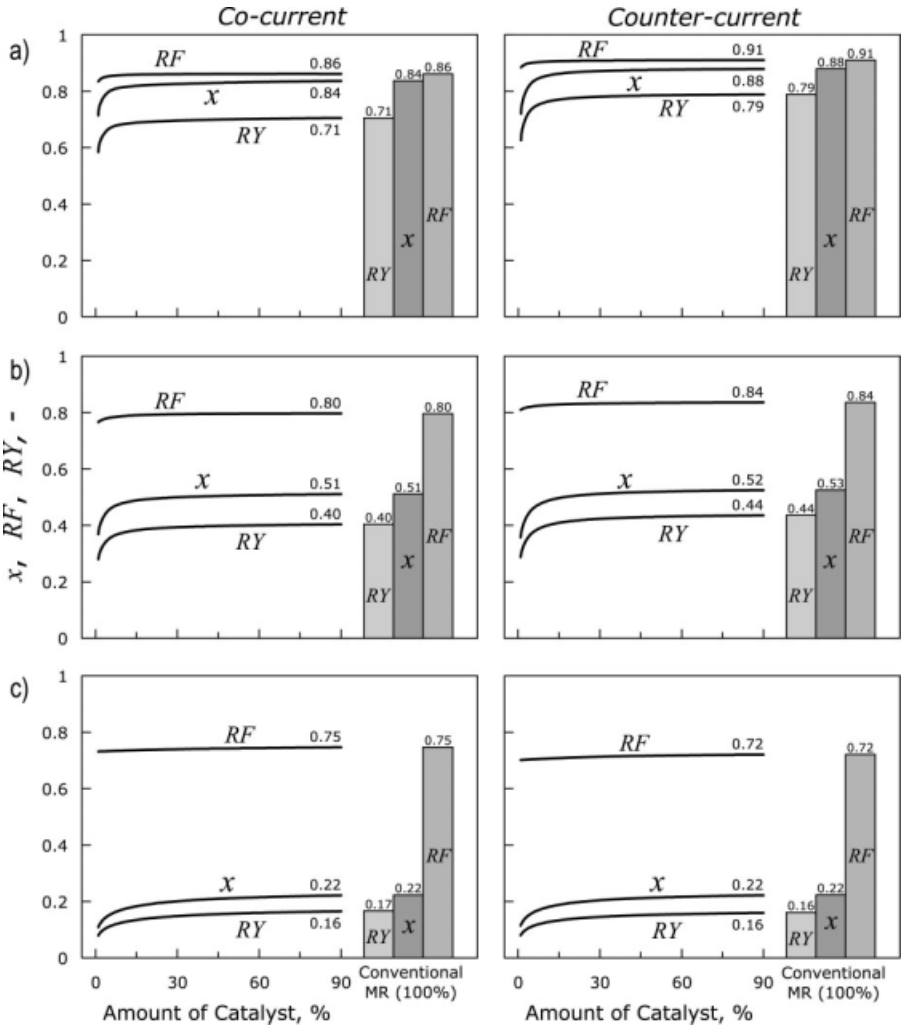


**Figure 11. Performances of the SMR ($CH_4$ conversion, $H_2$ recovery factor, and $H_2$ recovery yield) for $T^{Furnace}$ of 600°C (a), 500°C (b), and 400°C (c) in co- and counter-current flow at a "high" $n^{Stages}$ (=100) as a function of the catalyst fraction of the conventional MR, whose performances are also reported for comparison.**

The remaining operating conditions are specified in Table 3.

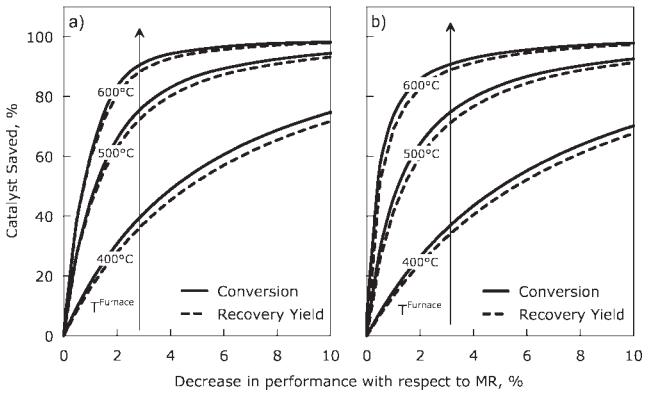


**Figure 12. Catalyst saved as a function of performance losses with respect to the conventional MR (in terms of methane conversion and hydrogen recovery yield) for different $T^{Furnace}$ in co- (a) and counter-current (b).**

The remaining operating conditions are specified in Table 3.

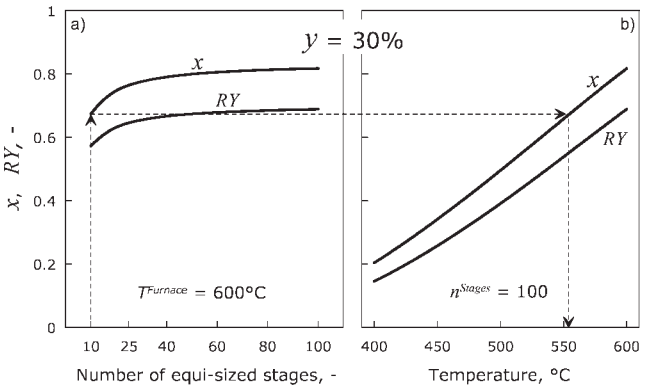


**Figure 14. Performance indices (a) as functions of $n^{Stages}$ at 600°C and (b) as functions of $T^{Furnace}$ for 100 stages in co-current flow.**

The dashed arrows (drawn only for conversion) indicate how to evaluate the advantage of adopting a high $n^{Stages}$ in terms of reduced $T^{Furnace}$.

theoretical considerations and, hence, represents an important result. Because also the plots for the conversion and recovery yield are very similar to each other at a given $T^{Furnace}$, the results can be summarized by considering the area encompassed between the lowest and the highest $x$ or $RY$ in co- or counter-current configurations. These relatively thin zones at each temperature constitute the Gain Map plotted in Figure 13. As an example of the savings significance, let us consider the case in which a performance gap of 1% in conversion or recovery yield is acceptable at a $T^{Furnace}$ of 600°C. The use of a staged reactor allows achieving the target performance and saving 67% of the catalyst used in a conventional MR.

Therefore, only one third of the catalyst mass can be utilized, with evident benefits in terms of cost of purchase, recovery and so on. If we tolerate a performance gap of 2%, the saved catalyst can reach 83%. From another perspective, the effect of $n^{Stages}$ can be analyzed in terms of a lower $T^{Furnace}$ that can be set for a given performance target. Figure 14 shows side-by-side the performance indices as functions of $n^{Stages}$ at 600°C (Figure 14a) and as functions of the temperature using 100 stages (Figure 14b). For example, by selecting a reference SMR with 10 stages at 600°C, it is shown that a 100-stage reactor operating at about 550°C can produce the same conversion. In such plots, $y$ is fixed (in this example 30%) and the same performance reproduced at an increased $n^{Stages}$ and a lower $T^{Furnace}$.

If we carry out a set of calculations with a varying $y$ and plot the temperature difference vs. $y$, we can build a map (Figure 15) analogous to Figure 13, where again a similar trend is

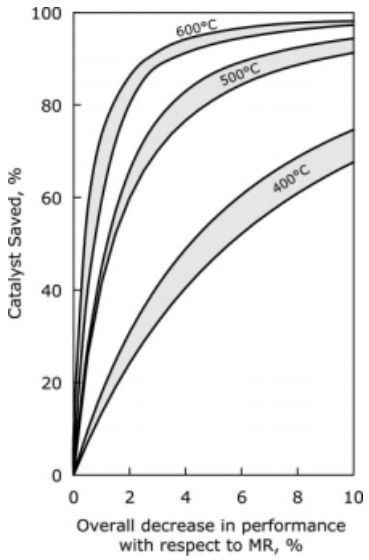


**Figure 13. Gain map for methane steam reforming carried out in a SMR.**

The remaining operating conditions are specified in Table 3.

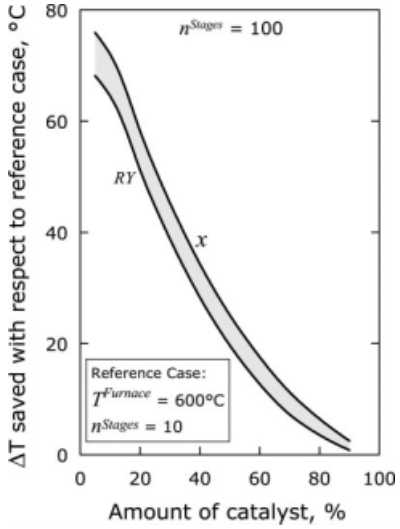


**Figure 15. Difference of $T^{Furnace}$ that is possible to save with respect to the reference case (600°C and 10 stages) by adopting a high $n^{Stages}$ (100) as function of $y$ for conversion and recovery yield.**

observed when fixing the conversion or the recovery yield. Figure 15 shows that the advantage in using a high $n^{Stages}$ decreases continuously with $y$. Considering that the performance indices of the reference case increase with $y$, the staged distribution has progressively less influence, as the reactor behavior tends to the one of the conventional MR. Using a lower $y$, $T^{Furnace}$ differences of various tens can be set if a sufficiently high $n^{Stages}$ is used. Together with the analysis made in terms of catalyst mass, i.e. more related to fixed costs, this result can be useful to reduce the heat requirement of the furnace, thereby decreasing the operating costs.

## Conclusions

In the present article the performances of a staged Pd-MR for the methane steam reforming process are investigated by computer simulations, focussing on the influence of the number of stages, and catalyst amount. The MR with reactive and inert stages in series is demonstrated to yield a methane conversion and hydrogen recovery yield comparable with the ones of a conventional MR but using only a fraction of its catalyst mass. Furthermore, it has been shown that the SMR with a high number of stages achieves performances similar to a reactor with the same catalyst uniformly diluted with inert particles. This result is demonstrated for different furnace temperatures and under co- and counter-current flow configurations. Catalyst savings of about 70% of the total can be achieved by giving up only 2% of the conversion or the recovery of a conventional MR. The catalyst amount savings vs. the gap of performances is quantified by means of an appropriate gain map. A similar analysis allowed deriving a map of the savings in terms of reduced furnace temperature as a function of the relevant performance loss. It is shown that these energy savings are significant as the number of stages increases.

## Acknowledgments

A. Caravella is grateful to the Repubblica Italiana, Ministero dell'Università e della Ricerca (MiUR) for the financial support in the frame of the Center of Excellence CEMIF.CAL (CLAB01TYEF). This work is part of the FIRB-CAMERE (RBNE03JCR5) project, funded by the "Ministero dell'Università e della Ricerca (MiUR)" that is gratefully acknowledged.

## Notation

$l$ = length (m)
$y$ = fraction of catalyst in the reactor (−, %)
$x$ = methane conversion (−)

### *Greek letters*

$\delta$ = thickness (m)
$\varepsilon$ = voidage degree of the catalytic and inert packs (−)

### *Superscripts*

Tot = Total (referred to the reactor length)
$R$ = Reactive (referred to the reactor stages)
$I$ = Inert (referred to the reactor stages)

### *Acronyms*

MR = (conventional) membrane reactor
SMR = staged membrane reactor
RF = hydrogen recovery factor (−)
RY = hydrogen recovery yield (−)

## Literature Cited

1. Caravella A, Di Maio FP, Di Renzo A. Computational study of staged membrane reactor configurations for methane steam reforming. I. Optimization of stage lengths. *AIChE J*. 2010;56(1): 248–258.
2. Åsen KI, Andersen HS. Method for manufacturing a hydrogen and nitrogen containing gas mixture, International Patent application no. WO 02/072470 A1, 2002.
3. Birdsell SA, Willms RS. Tritium recovery from tritiated water with a two-stage palladium membrane reactor. Fusion engineering and design. Proceeding Acts of ISFNT 4: International Symposium on Fusion Nuclear Technology No. 4, Tokyo, Japan, 1998;39–40:1041–1048.
4. Lund CRF. Water-gas shift kinetics over iron oxide catalysts at membrane reactor conditions. Final report. Chemical Engineering Department, University at Buffalo, SUNY-Buffalo, NY, 2002.
5. Patil CS. Membrane reactor technology for ultrapure hydrogen production, PhD Thesis, University of Twente, Twente, The Netherlands, 2005. ISBN: 9036522463.
6. Li A, Lim CJ, Grace JR. Staged-separation membrane reactor for steam methane reforming. *Chem Eng J*. 2008;138:452–459.
7. Jordal K, Bredesen R, Kvamsdal HM, Bolland O. Integration of $H_2$-separating membrane technology in gas turbine processes for $CO_2$ capture. *Energy*. 2004;29:1269–1278.
8. Caravella A, Di Maio FP, Di Renzo A. Optimization of membrane area and catalyst distribution in a permeative-stage membrane reactor for methane steam reforming. *J Membr Sci*. 2008;321:209–221.
9. Xu J, Froment GF. Methane steam reforming, methanation and water-gas shift. I. Intrinsic kinetics. *AIChE J*. 1989;35:88–96.
10. Xu J, Froment GF. Methane steam reforming, methanation and water-gas shift. II. Diffusional limitations and reactor simulation. *AIChE J*. 1989;35:97–103.
11. Tong J, Matsumura Y, Suda H, Haraya K. Experimental study of steam reforming of methane in a thin (6 $\mu$m) Pd-based membrane reactor. *Ind Eng Chem Res*. 2005;44:1454–1465.
12. Tong J, Matsumura Y. Thin Pd membrane prepared on macroporous stainless steel tube filter by an in-situ multi-dimensional plating mechanism, *Chem Commun*. 2004;2004:2460–2461.

*Manuscript received Dec. 10, 2008, and revision received Apr. 6, 2009.*